Journal of Nanostructure in Chemistry (2019) 9:175–187
https://doi.org/10.1007/s40097-019-0308-7

ORIGINAL RESEARCH

Inhibitive effect of super paramagnetic iron oxide nanoparticles on the alkaline hydrolysis of procaine

Kashif Raees[1] · Mohd Shaban Ansari[1] · M. Z. A. Rafiquee[1]

Received: 19 March 2019 / Accepted: 5 June 2019 / Published online: 17 June 2019

Abstract

The Super Paramagnetic Iron Oxide Nanoparticles (SPIONs) can bind drugs and act as drug-carriers. The magnetically active SPIONs can be used to deliver the drugs to the target through magnetic fields. The objective of the present work has been undertaken to study the stability, and binding behaviour of procaine with SPIONs and surfactant-coated SPIONs. Procaine is among the ester drugs and hydrolyses in the alkaline medium. The influence of SPIONs and surfactant-coated SPIONs on the rate of hydrolysis of procaine in alkaline medium may help to define the behaviour of the drug in the presence of these nanoparticles. The kinetic studies of procaine hydrolysis in the presence of SPIONs and surfactant-coated SPIONs were carried out spectrophotometrically. The concentrations of OH^- ions were taken in excess over [procaine] to keep the reaction conditions under pseudo-first-order. The presence of SPIONs and the SPIONs coated with cetyltrimethylammonium bromide; CTABr and sodium dodecylsulphate; SDS surfactants displayed an inhibitive effect on the rate of hydrolysis of procaine. The synthesised nanoparticles were characterised using X-ray diffraction (XRD), scanning electron microscopy (SEM), vibrating sample magnetometer (VSM), transmission electron microscopy (TEM) and Fourier transform infrared spectroscopy (FTIR). The k_{ψ}-[surfactant] profile in the presence of SPIONs was discussed using the pseudophase model in which the reactants are considered to be distributed in the aqueous and micellar media. The rate constant for the procaine hydrolysis and the binding constants of procaine with coated and non-coated SPIONs have been calculated by analysing the data for the variation in the rate constant with the change in [surfactant], [SPIONs] and [surfactant-coated SPIONs].

Extended author information available on the last page of the article

Graphic abstract

The studies on the rate of hydrolysis of procaine in the presence of SPIONs and surfactant-coated SPIONs shows inhibitive effects of NPs on the reaction. Procaine has good binding affinity with surfactant-coated SPIONs in comparison with the bare SPIONs.

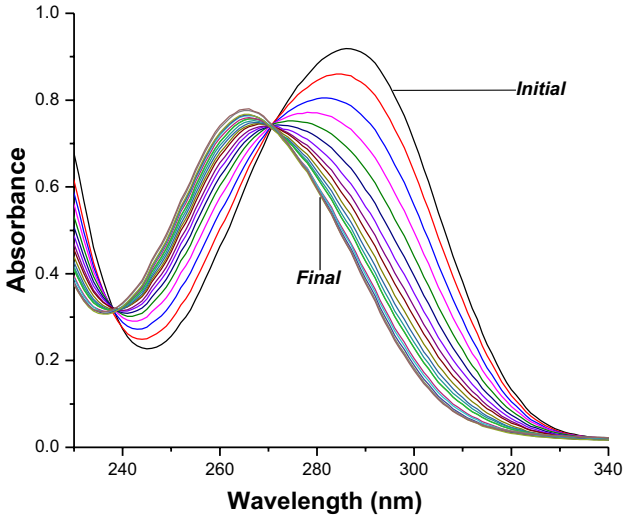

Keywords Base-catalysed hydrolysis of procaine · SPIONs · CTABr · SDS · Surfactant-coated SPIONs

Introduction

Superparamagnetic iron oxide nanoparticles (SPOINs) are inert, almost inexpensive, biocompatible, having unmatched magnetic properties, and can be reused or recycled using simple magnets [1–3]. SPIONs find applications in the fields of chemical catalysis, magnetic fluids, magnetic seals, data storage and various bio-applications like clinical diagnosis and therapy (such as MRI and MFH), biological labels, magnetic bio-separation and targeted drug delivery [4–9]. The SPIONs give the freedom to control the morphology, shape and size of the nanoparticles during the synthesis process, which can be used further in different applications [10–13]. The surface of iron oxide nanoparticles can be modified or coated as per need using various polymers, surfactants and inorganic materials like silica [14–18]. These nanocatalysts have successfully been used for catalysing the organic reactions like carbon–carbon coupling reactions, oxidations, epoxidation reactions and hydro-formylation reactions. [19–21]. Magnetic nanoparticles are synthesised using different methods like thermal decomposition, microemulsion, and co-precipitation [22–24]. Among these methods, the co-precipitation of ferrous and ferric salts is the most widely accepted method because of its reliability, low cost, and high yield. The ability of surfactants to change the detergency, wettability and foaming behaviour of the solution makes it useful in the field of medicines, detergents, paints, coatings, home and personal care products, enhanced oil recovery and in pharmaceuticals [25]. When dissolved in polar solvents like water, surfactant molecules aggregate to form micelles above its critical micelles concentrations (CMC). The micelles provide a different microenvironment and affect the rate of hydrolysis reaction.

The surfactant-coated SPIONs present a different microstructure and may influence the rate of reactions in a manner different than the micellar aggregates. The micelles present the ionic or polar surface and non-polar core. The molecules bind with the micelles from the stern region to the inner core, depending upon its polarity. The investigations on the rate of procaine hydrolysis by surfactant molecules encapsulating the SPIONs may help to establish the nature of binding between surfactant and procaine at the molecular level. Procaine (2-diethylaminoethyl-4-aminobenzoic acid) is among the most widely accepted ester-based local anaesthetic drug. Procaine hydrochloride injections have been used in infiltration anaesthesia, spinal anaesthesia, peripheral nerve block and some severe pain conditions such as Bell's palsy, Scalenous Anticus syndrome, arthritis, and cerebral thrombosis. The primary issue with procaine is its lower shelf life while storage and its lower duration of action when injected in a patient's body. Loucas et al. have reported a 90% decrease in the initial concentration of procaine in 11 days under refrigeration and just 2 days at room temperature [26]. Several researchers have made

efforts to increase the shelf life or stability of procaine using certain additives like surfactants, natural polymers or other drugs [27]. Here, we are trying a different method using SPIONs to lower down procaine's rate of degradation and hence, increase its stability. The kinetics experiments in the presence of non-coated and coated SPIONs have been carried out and presented here.

Experimental

Materials

Procaine hydrochloride with 98% purity was purchased from TCI, Tokyo, Japan. Ferric chloride (97%), ferrous chloride dihydrate (99%), SDS (99%) and CTABr (99%) were purchased from CDH, New Delhi, India. Liquor ammonia 25% with a purity index of 99% was purchased from Thermo Fisher Scientific, Mumbai, India and sodium hydroxide with 97% purity was purchased from Merck, Mumbai, India to perform the experiments.

The stock solutions of procaine hydrochloride were prepared in 99.9% ethanol and used within a week, rest all other solutions were made in double distilled water.

Synthesis of SPIONs

The SPIONs used in the present study were synthesised in the research lab using the co-precipitation method by taking 20.0 g of $FeCl_3$ (0.4 M) and 10.0 g of $FeCl_2{\cdot}2H_2O$ (0.2 M) in a 1000 mL conical flask containing 300 mL double-distilled water. For CTABr- and SDS-coated SPIONs, 0.2 M of CTABr or SDS solutions were mixed during co-precipitation of iron salts. The mixture was then de-oxygenated by purging N_2 gas and stirred vigorously for 60 min to ensure complete mixing of Fe^{3+} and Fe^{2+} ions. Co-precipitation of iron salts was carried out by adding 200 mL liquor ammonia (25%) dropwise in the conical vessel. An inert environment was maintained by continuously purging the N_2 gas in the reaction vessel and over the surface of the mixture to ensure the synthesis of magnetite (Fe_3O_4). The pH of the reaction medium then rose to above 10 by adding 2 M of NaOH solution dropwise. The higher pH (10–14) ensures the complete precipitation of iron salts as well as decreases the size of nanoparticles. The temperature was then raised to 70 °C with continuous stirring and purging N_2 gas for 5 h. The precipitate obtained was then filtered, washed with acetone and double-distilled water until the pH comes to neutral, and then dried for 5–6 h at 70 °C in a hot air oven. The synthesised magnetite nanoparticles were black, possessing very high magnetic behaviour. The overall reaction can be written as:

$$Fe^{2+} + 2Fe^{3+} + 8OH^- \rightarrow Fe_3O4 + 4H_2O.$$

The synthesised nanoparticles were characterised by X-ray diffraction using 'MiniFlex' II X-ray diffractometer from Rigaku, Japan, having a radiation source of CuKα with $\lambda = 1.5406$ nm. FTIR Spectrometer 'Nicolet iS50' from Thermo Fisher Scientific, Madison, USA was used to record the FTIR data of the synthesised nanoparticles. The magnetic behaviour of nanoparticles was measured using Vibrating sample magnetometer (VSM) MicroMag-3900 Princeton, USA.

Kinetic measurements

All kinetic measurements were made using a double-beam spectrophotometer 'GENESYS 10S UV/VIS' from Thermo Fisher Scientific, Madison, USA. A 3.0 mL quartz cuvette having 10 mm path length was used to measure the absorbance of the samples. The temperature at 37.0 ± 0.3 °C was kept constant by placing in water bath from Ferrotek Equipments, Ghaziabad, India. While performing the kinetic runs the reaction conditions were maintained under pseudo-first-order by keeping [NaOH] > > [procaine], and a decrease in absorbance for the hydrolysis of procaine was followed at a wavelength of 291 nm as a function of time. The solution containing procaine and NaOH at a respective concentration of 5.0×10^{-5} mol dm^{-3} and 5.0×10^{-2} mol dm^{-3} was scanned repetitively and recorded at an interval of 5 min and are presented in Fig. 1. The required amount of reactants was taken into a round-bottom flask and held in a water bath for around 30 min so that the procaine can equilibrate with surfactants and SPIONs. The reaction was started (zero time was taken) with the introduction of sodium hydroxide into the reaction flask. The kinetic measurements were set in the spectrophotometer at a time interval of 5 min, and the monitoring of the reaction was performed until the completion of at least three half-life periods. All kinetic runs were repeated thrice to minimise the random errors, and the reproducibility found for the observed values was within the error limit of ± 5%. The values of rate constant were calculated from the slope of the plots of ln (absorbance) versus time.

Results and discussion

Characterization of SPIONs

Scanning electron microscopy (SEM)

The surface features of the SPIONs, CTABr-coated SPIONs, and SDS-coated SPIONs are clearly shown by the SEM images in Fig. 2a–c, respectively, which indicates the successful synthesis of nanoparticles. The nanoparticles seem to have a nonspherical irregular shape in non-coated Fe_3O_4 and spherical shape when coated with CTABr and SDS.

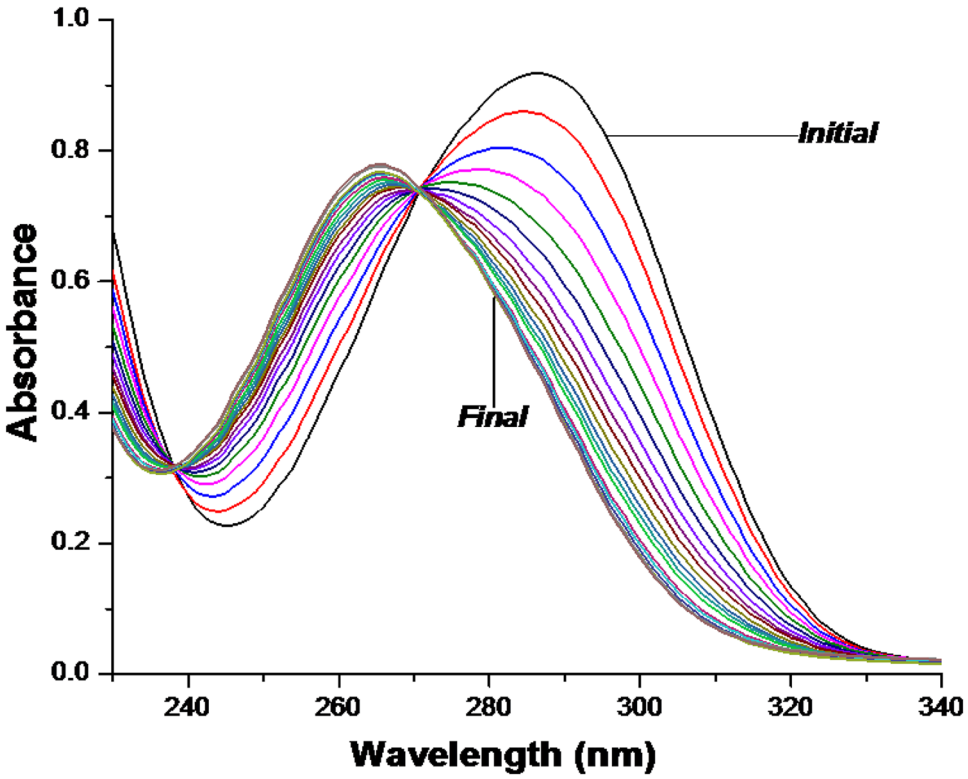

Fig. 1 Repetitive scans for the alkaline hydrolysis of procaine at an interval of 5 min. Reaction conditions: [procaine] = 5.0×10^{-5} mol dm^{-3}, [NaOH] = 5.0×10^{-2} mol dm^{-3}, Temperature = 37 °C

Transmission Electron Microscopy (TEM)

Figure 2a′–c′ shows the TEM images of synthesised SPIONs, CTABr-coated SPIONs and SDS-coated SPIONs, respectively. One thing that can be seen in the TEM images is that there is a kind of agglomeration in the non-coated SPIONs whereas in surfactant-stabilised SPIONs agglomeration is reduced to a certain extent.

X-ray diffraction (XRD)

The XRD results (Fig. 3a–c) obtained, confirmed the crystalline nature of synthesised coated and non-coated SPIONs. The diffraction peaks appeared at $2\theta = 30.26°$, 35.5°, 43.12°, 53.74°, 57.10° and 62.92° , respectively, correspond to (220), (311), (400), (422), (511), and (440) planes. The broad peaks indicate the ultrafine nature and small crystalline size of the Fe_3O_4 particles having the cubic structure [28].

Fourier transform infrared spectroscopy (FTIR)

Figure 4a–c shows the FTIR spectra of SPIONs, CTABr-coated SPIONs and SDS-coated SPIONs, respectively. The peaks at 3424 cm^{-1}, 3430 cm^{-1} and 3431 cm^{-1} in (a), (b), and (c), respectively, are due to O−H stretching vibration arising from the hydroxyl group which is likely due to the adsorption of water molecules on the surface of SPIONs. The peaks at 2920 cm^{-1} and 2850 cm^{-1} in (b) and at 2922 cm^{-1} and 2854 cm^{-1} in (c) are attributed to CH bands' vibrations of the $–CH_2$ group in CTABr and SDS. The H–O–H bending of H_2O molecules is also localised at 1631 cm^{-1}, 1630 cm^{-1}, and 1635 cm^{-1} in (a), (b) and (c), respectively [29]. The peaks appearing at 1465 cm^{-1} in (b) and 1460 cm^{-1} in (c) correspond to the $-CH_2$ group's bending vibrations in CTABr and SDS. The peaks at 1220 cm^{-1} and 964 cm^{-1} in (c), respectively, correspond to S=O stretching vibrations and out-of-plane bending vibrations of C–H bond. The peaks at 585 cm^{-1} and 435 cm^{-1} in (a), 566 cm^{-1} and 475 cm^{-1} in (b) and 547 cm^{-1} and 474 cm^{-1} in (c) correspond to the Fe−O bonds in magnetite and the two peaks affirm the spinal structure of magnetite nanoparticles [30]. The difference in the Fe−O bond-lengths in Fe_3O_4 molecules is the reason for two peaks for a single Fe−O bond.

Vibrating sample magnetometer (VSM)

The magnetic behaviour of the SPIONs and surfactant-coated SPIONs has been studied using VSM. The saturation magnetisation of nanoparticles was observed at 71.82 emu/g in non-coated SPIONs (Fig. 5), which indicates a very high saturation magnetisation and superparamagnetic behaviour [31].

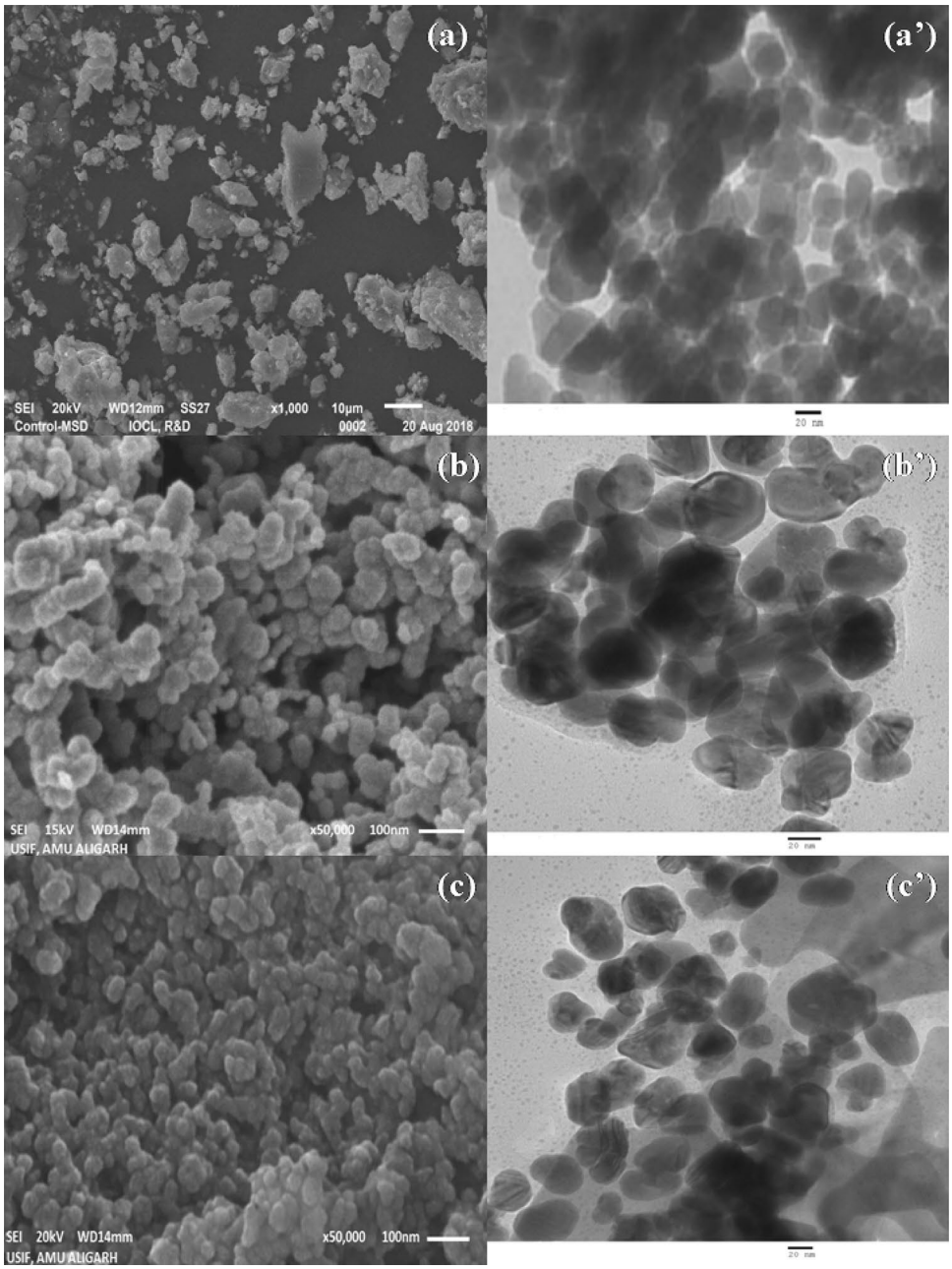

Fig. 2 **a**, **b** and **c** are SEM and (**a′**), (**b′**) and (**c′**) are TEM images of synthesised Fe_3O_4, CTABr-coated Fe_3O_4- and SDS-coated Fe_3O_4 nanoparticles

Hydrolysis of procaine in aqueous medium

The rate of procaine hydrolysis catalysed by OH^- ions to yield *N,N*-diethyl amino-ethanol and p-amino-benzoate anion in the aqueous medium is given by the following rate equation [32]:

$$\text{rate} = -\frac{\mathrm{d}[\text{procaine}]}{\mathrm{d}t} = k_1[\text{procaine}]\,[\text{OH}^-], \tag{1}$$

where k_1 is the first-order rate constant. The rate of reaction depends upon $[OH^-]$ and is independent on [procaine]

$$\text{or, Rate} = k_{\text{obs}}[\text{procaine}]_{\text{T}}. \tag{2}$$

The values of k_{obs} are related to the second-order rate constant (k_2) as given by Eq. (3).

$$k_{\text{obs}} = k_2[\text{NaOH}]. \tag{3}$$

The plot of k_{obs} against [NaOH] gave straight line (Fig. 6), a similar trend was observed following the earlier studies [33, 34], and the value of k_2 was obtained from the slope of the plot.

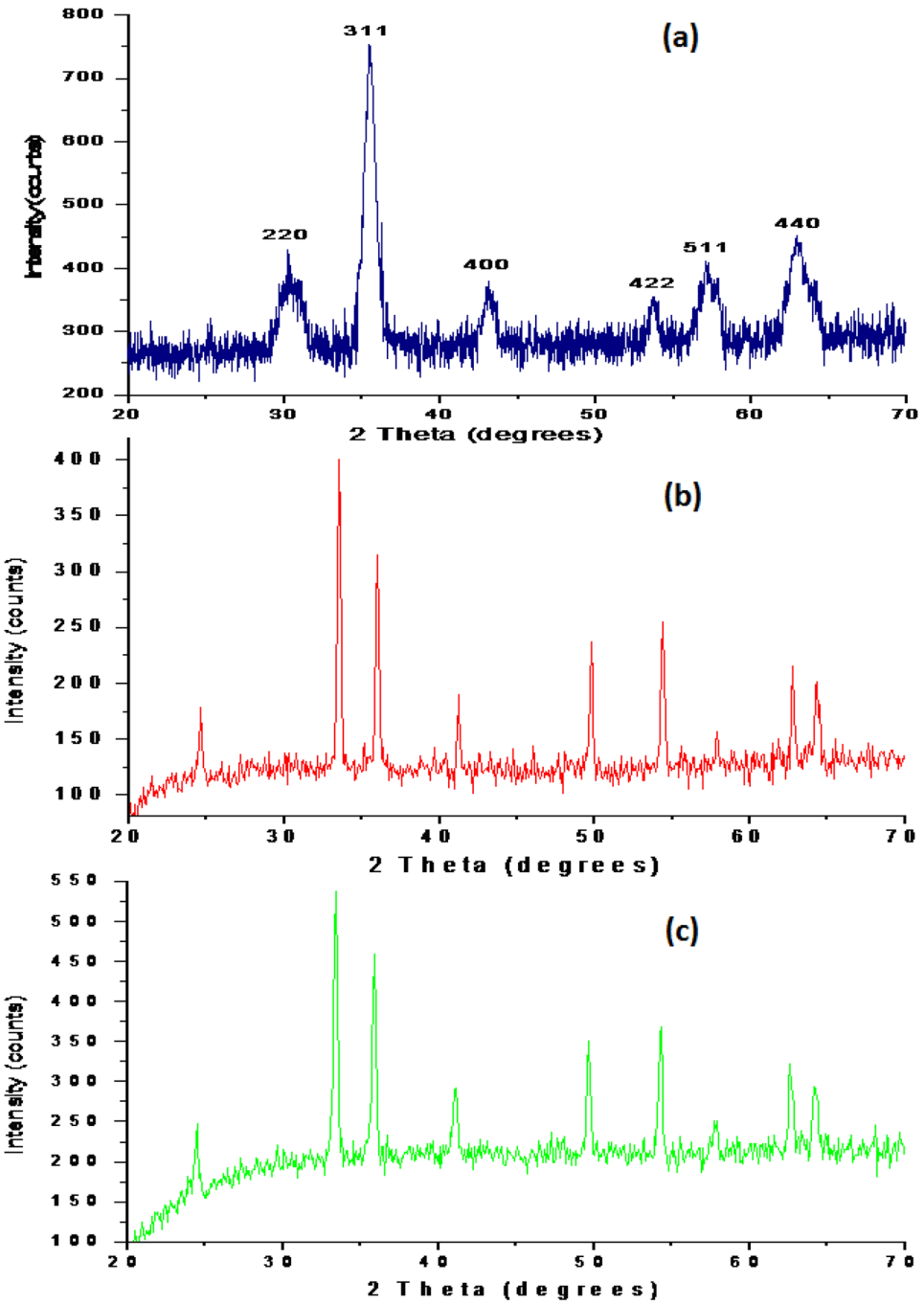

Fig. 3 X-ray diffraction patterns of the synthesised Fe_3O_4 (**a**), CTABr-coated Fe_3O_4 (**b**), and SDS-coated Fe_3O_4 (**c**) nanoparticles

Influence of micelles on the rate of hydrolysis of procaine

The [SDS] and [CTABr] varied in the concentration range from 1.0×10^{-2} mol dm^{-3} to 5.0×10^{-2} mol dm^{-3}, and their influence on the values of rate constants was studied. The rate constant values found to decrease with increase in the concentration of surfactants (Figs. 7, 8). SDS showed more significant inhibition on the rate of hydrolysis than CTABr. At a concentration higher than the CMC values, these surfactant molecules exist in the associated form (micelles), and procaine gets distributed between the micellar and aqueous pseudophases. The relative amount of procaine in these two phases (called binding constant 'K_s') depends upon the nature of the drug and the charge on the micelles. The hydrolysis of procaine by NaOH in micellar solutions is assumed to occur in both micellar as well as in aqueous pseudophases. The following Scheme 1 represents the mechanism of the hydrolysis reaction in the micellar media:where, k'_w and k'_m, respectively, denote the

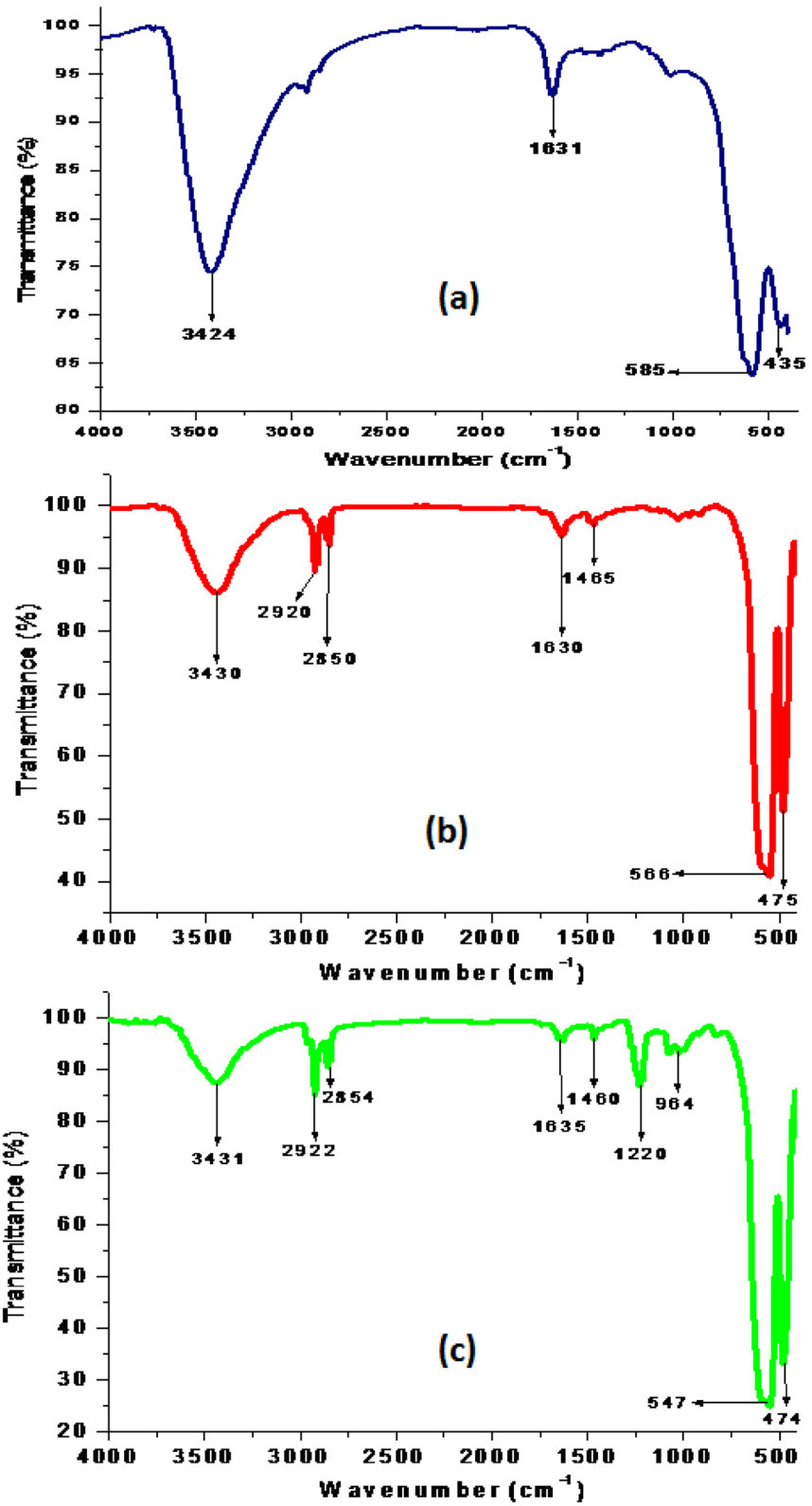

Fig. 4 FTIR spectra of the synthesised Fe_3O_4 (**a**), CTABr-coated Fe_3O_4 (**b**), and SDS-coated Fe_3O_4 (**c**) nanoparticles

first-order rate constants for the reaction taking place in aqueous and micellar pseudophases; S_w is the equilibrium concentration of procaine in aqueous phase; S_m represents the concentration of the drug in micellar phase, and D_n represents the concentration of micelles. The reaction rate correlates with Scheme 1 is given by Eq. (4):

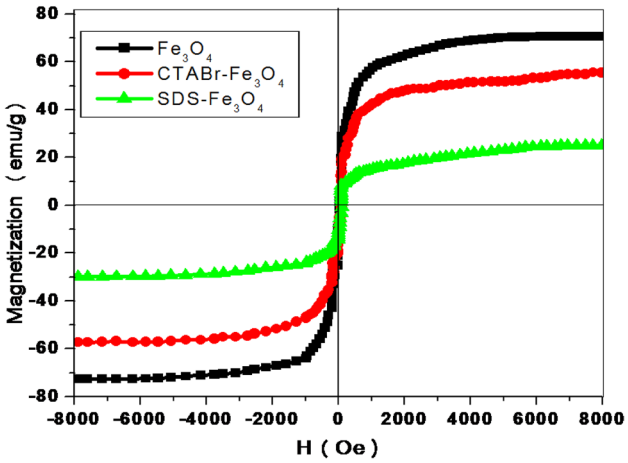

Fig. 5 Hysteresis curves of coated and non-coated SPIONs at room temperature

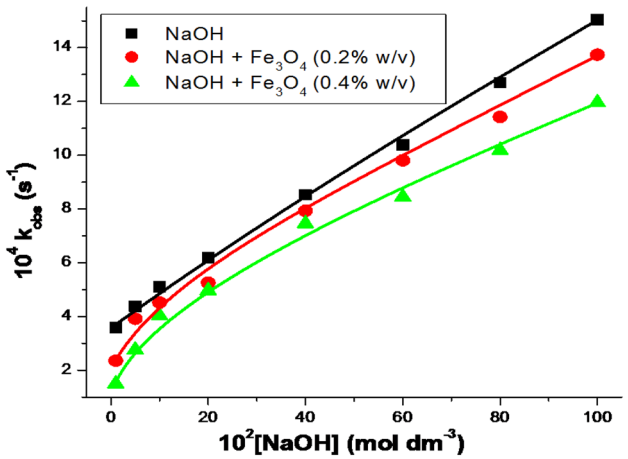

Fig. 6 Plot of observed values of rate constant (k_{obs}) versus [NaOH]. Reaction conditions: [Procaine] = 5.0×10^{-5} mol dm^{-3}, temperature = 37 °C

$$\text{rate} = \frac{k'_w + k'_m K_s [D_n]}{1 + K_s [D_n]} [S_T] = k_\psi [S_T], \quad (4)$$

$$\text{where} \quad k_\psi = \frac{k'_w + k'_m K_s [D_n]}{1 + K_s [D_n]}. \quad (5)$$

The cationic (CTABr) and anionic (SDS) micelles are found to inhibit the hydrolysis of procaine. The hydrolysis reaction was initiated when the carboxyl carbon of the ester group was attacked by the OH^- ions, forming the tetrahedral intermediate. The local concentration of OH^- ions in the micellar regions of CTABr and SDS plays an important role on the reaction rate. The OH^- ions are present around

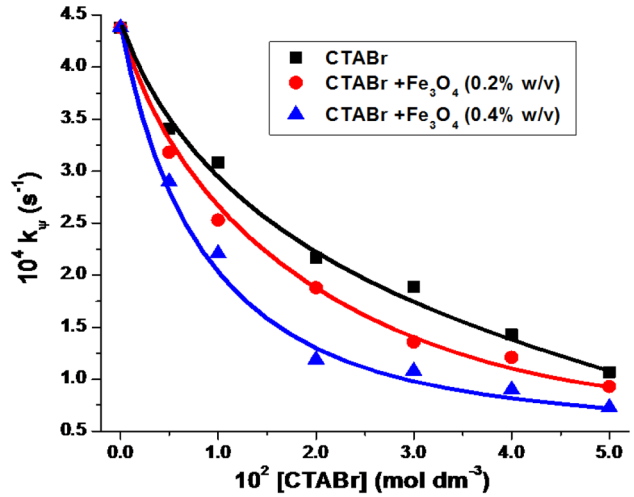

Fig. 7 Plots of k_ψ versus [CTABr] in the absence and presence of Fe_3O_4. Reaction conditions: [procaine] = 5.0×10^{-5} mol dm^{-3}, [NaOH] = 5.0×10^{-2} mol dm^{-3} and temperature = 37 °C

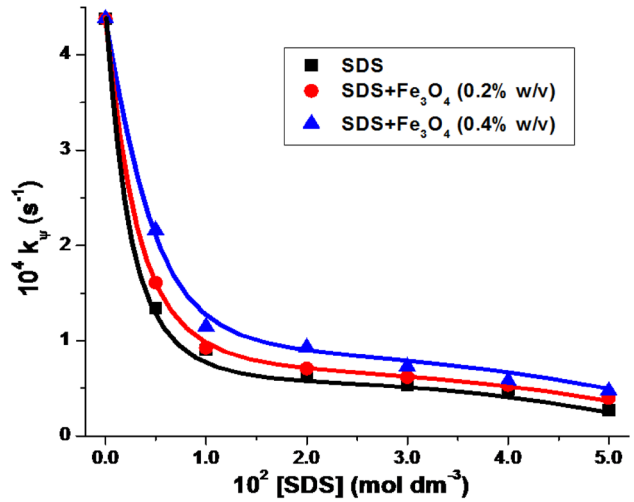

Fig. 8 Plots of k_ψ versus [SDS] in the absence and presence of Fe_3O_4. Reaction conditions: [procaine] = 5.0×10^{-5} mol dm^{-3}, [NaOH] = 5.0×10^{-2} mol dm^{-3} and temperature = 37 °C

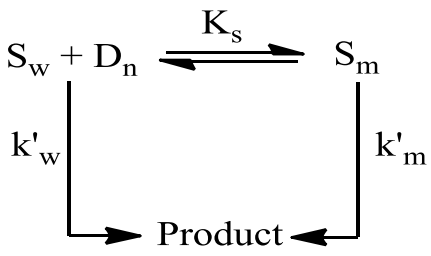

Scheme 1 .

CTA^+ micelles as the counter ions by displacing some of the Br^- ions, depending upon the values of the equilibrium constant for the exchange of ions, K_{Br}^{OH}. The following Eqs. (6–7) give the equilibrium distribution of OH^- ions on the micellar surface.

$$OH_w^- + Br_m^- \rightleftharpoons OH_m^- + Br_w^-, \tag{6}$$

$$\text{Or,} \quad K_{Br}^{OH} = \frac{[OH_m^-][Br_w^-]}{[OH_w^-][Br_m^-]}. \tag{7}$$

The subscript w represents the OH^- ions in the aqueous and m represents the Br^- ions in the micellar pseudophases. The values of rate constant with respect to the total concentration of OH^-, CTABr, and second-order micellar (k_m) and aqueous (k_2) rate constant, is given by Eq. (8):

$$k_\psi = \frac{k_2[OH_T^-] + (k_m K_s - k_2) m_{OH}[D_n]}{1 + K_s[D_n]}, \tag{8}$$

where m_{OH} represent the molality of hydroxide ions bonded with surfactant as a counter ion. The value of m_{OH} is obtained on solving the quadratic Eq. (9). The values of β (=0.8) were taken from the literature [35], and different values of K_{Br}^{OH} were regressed to determine the m_{OH} which, further, gave the values of K_s and k_m [Eq. (8)] with least standard deviation values. The values of K_s and k_m are given in Table 1

$$m_{OH}^2 + m_{OH}\left[\frac{[OH_T^-] + K_{Br}^{OH}[Br_T^-]}{(K_{Br}^{OH} - 1)[D_n]} - \beta\right] - \frac{\beta[OH_T^-]}{(K_{Br}^{OH} - 1)[D_n]} = 0. \tag{9}$$

The inhibitive effect shown by SDS is because the procaine molecules get partitioned in the anionic micelles and aqueous pseudophases. The organic moieties of procaine drag the molecules more in the region of lower polarity (i.e. in the micellar pseudophase) than the polar aqueous pseudophase, whereas, the concentration of OH^- ions is expected to be low in the region of DS^- micellar surface and more in the aqueous phase. The similar charges on the DS^- micellar surface and OH^- ions cause the dilution of OH^- ions on the micellar surface region. Since the procaine mainly hydrolysed in the aqueous phase, therefore, the pseudophase model is applied to get the following Eq. (10).

$$\frac{1}{k'_w - k_\psi} = \frac{1}{k'_w - k'_m} + \frac{1}{(k'_w - k'_m) K_s [D_n]}. \tag{10}$$

The K_s and k'_m have been obtained from the plot of $\frac{1}{k'_w - k_\psi}$ versus $\frac{1}{[D_n]}$ and are given in Table 2. On increasing the concentration of surfactants, the amount of micelles also increases, causing a decrease in the procaine concentration in aqueous pseudophase, and thus, the rate of reaction decreases.

Effect of SPIONs on the hydrolysis of procaine

The addition of SPIONs into the reaction mixture of NaOH and procaine cause a dip in the rate of reaction. The kinetic studies carried out at 0.2% and 0.4% (*w*/*v*) SPIONs with varying concentration of sodium hydroxide ranging from 2.0×10^{-2} mol dm^{-3} to 1.0 mol dm^{-3} (Fig. 6) reveal that the values of k_{obs} increased on increasing the [NaOH]. The influence of varying quantity of SPIONs [from 0.02% to 0.40% (*w*/*v*)] on the rate of reaction was studied at four different NaOH concentrations (i.e. 5.0×10^{-2} mol dm^{-3}; 2.0×10^{-1} mol dm^{-3}; 4.0×10^{-1} mol dm^{-3}; and 6.0×10^{-1} mol dm^{-3}). At each [NaOH], the values of rate constant are lower at different amount of Fe_3O_4 as given in Fig. 9. Based on these experiments, it is inferred that the presence of Fe_3O_4 slows the rate of reaction. The lowering in the velocity of procaine hydrolysis in the presence of SPIONs may be due to the adsorption of procaine, OH^- ions or both on the surfaces of SPIONs, causing an inhibitive effect on the reaction. The Fe_3O_4 adsorbs OH^- ions and procaine through the lone pairs of electrons available on the oxygen of ester group. The adsorption of OH^- ions on the surface of SPIONs occurs through the electrostatic bonding, whereas the adsorption of procaine takes place through the oxygen atom of SPIONs to the ester carbon atom via coordinate bonding. The adsorption of procaine on the SPIONs surface through

Table 1 Fitting values of K_s and k_m obtained from the plots of k_ψ versus $[D_n]$ for CTABr

Kinetic parameters	Values
K_{Br}^{OH}	14
β	0.8
$10^4 k_2$ (mol^{-1} dm^3 s^{-1})	8.76
K_s	1800 ± 20
10^4 k_m (mol^{-1} dm^3 s^{-1})	7.94 ± 0.6

Reaction conditions: [procaine] = 5.0×10^{-5} mol dm^{-3}, [NaOH] = 5.0×10^{-2} mol dm^{-3} and temperature = 37 °C

Table 2 Values of K_s and k_m obtained from the plots of $\frac{1}{k'_w - k_\psi}$ versus $\frac{1}{[D_n]}$ for SDS

Kinetic parameters	Values
K_s	3690
10^5 k_m (s^{-1})	5.41
R^2	0.957

Reaction conditions: [procaine] = 5.0×10^{-5} mol dm^{-3}, [NaOH] = 5.0×10^{-2} mol dm^{-3} and temperature = 37 °C

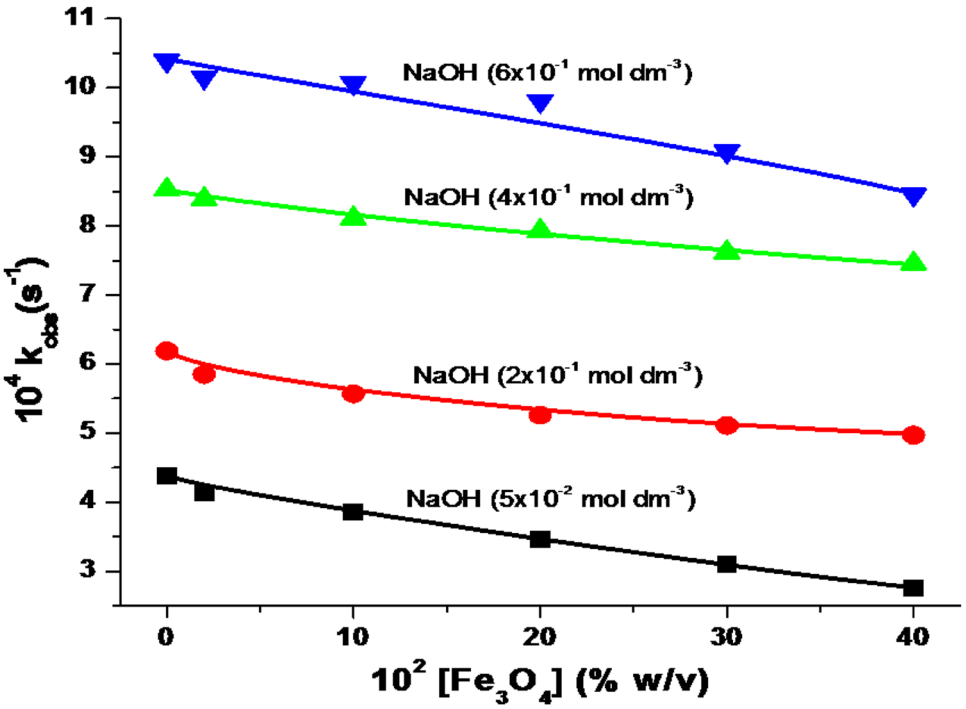

Fig. 9 Plot of observed values of rate constant (k_{obs}) versus [Fe_3O_4] at different NaOH concentrations. Reaction conditions: [procaine] = 5.0×10^{-5} mol dm^{-3}, temperature = 37 °C

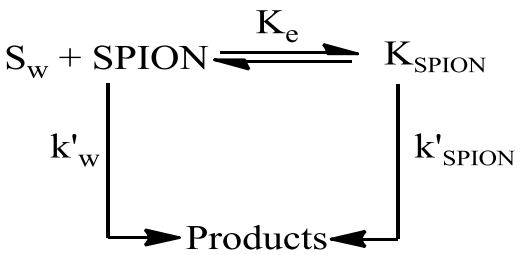

Scheme 2 .

Table 3 Values of K_e obtained from the plots of $\frac{1}{k'_w - k_{SPION}}$ *versus* $\frac{1}{[SPION]}$ at different [NaOH]

10^2 [NaOH] (mol dm^{-3})	K_e
5.0	10.20
20	5.37
40	2.75
60	0.73

Reaction conditions: [procaine] = 5.0×10^{-5} mol dm^{-3} and temperature = 37 °C

the ester carbon atom makes it unavailable for the OH^- ions' attack and thereby decreases the rate of reaction. The mechanism similar to Scheme 1 can be proposed to describe the reaction in the presence of SPIONs in the following Scheme 2.

The increase in OH^- ions makes the SPIONs' surfaces more saturated and neutralised due to which the tendency of SPIONs to form complex with ester carbon of procaine decreases. The increase in SPIONs shifts the equilibrium more towards the formation SPIONs–procaine complex and, therefore, the rate of reaction decreases on increasing the [SPIONs]. The rate Eq. (11), corresponding to the mechanism in Scheme 2, was used to calculate the equilibrium constant (K_e) for the binding between procaine and SPIONs

$$\frac{1}{k'_w - k_{SPION}} = \frac{1}{k'_w - k'_{SPION}} + \frac{1}{(k'_w - k'_m)K_e[SPIONs]}. \quad (11)$$

The values of the rate constant (k'_{SPION}) and equilibrium constant (K_e) for the hydrolysis of procaine in the presence of SPIONs were calculated from the plot of $\frac{1}{k'_w - k_{SPION}}$ versus $\frac{1}{[SPIONs]}$ and the values obtained are shown in Table 3. The table clearly shows that the equilibrium constant values decrease with increase in [OH^-] ions and therefore, the reaction rate increases with an increase in [OH^-] ions. These observations are in a similar line to the earlier studies, in which the adsorption to the various metal oxides causes a decrease in the rate of reactions [36].

The addition of surfactants (CTABr and SDS) into the reaction mixture comprising, procaine, NaOH, and SPIONs caused a decrease in reaction rate. The surfactants' concentrations were varied in the range from 2.0×10^{-3} mol dm^{-3} to 5.0×10^{-2} mol dm^{-3} at 0.2% and 0.4% (w/v) SPIONs. Under these reaction conditions, the reactant procaine is now distributed into aqueous and micellar phases and also adsorbed to SPIONs surfaces. Consequently, a slight edge on the inhibition of the rate of procaine hydrolysis is

observed in the case of CTABr (Fig. 7). It is also likely that CTABr enhances the extent of adsorption to the SPIONs surface through binding of the oxygen of the ester group with quaternary ammonium of CTABr molecule, which results in the shift of equilibrium towards the formation of the SPION–procaine complex. The synergistic effect of the surfactant molecules in binding the procaine with SPIONs surfaces further decreases the rate of hydrolysis.

Contrary to the effect of CTABr on the hydrolysis rate, the variation in [SDS] at fixed [NaOH] increased the rate of hydrolysis in the presence of 0.2% and 0.4% (w/v) SPIONs (Fig. 8). The rise in the rate of reaction in the presence of SDS–SPIONs is supposed to be due to the weak binding of procaine with SDS–SPIONs surface. The lower binding ability for procaine with SDS–SPIONs shifts the equilibrium more towards the aqueous medium, and therefore, an increase in the hydrolysis rate is observed. The lower binding of procaine with SDS–SPIONs may also be due to the more competitive binding of OH^- ion with anionic SDS-coated SPIONs, and thus, procaine remains mostly in the aqueous phase.

To study the binding behaviour of surfactant (CTABr and SDS) at the molecular level, these surfactant-coated SPIONs (in different amounts) were added to the reaction mixture containing procaine and NaOH. Figure 10 shows a steep decrease in the rate of hydrolysis on increasing the quantity of surfactant-coated SPIONs in the reaction mixture. The maximum inhibitive effect observed for the SPIONs coated with SDS. The results treated in light of Scheme 2 and Eq. (11), and the obtained values of equilibrium constant are presented in Table 4. The equilibrium constant value for the binding of procaine with SDS was found to be higher than with CTABr. It may be likely that the SDS–SPIONs at the molecular level in the absence of micelles adsorb more procaine through hydrophobic interactions.

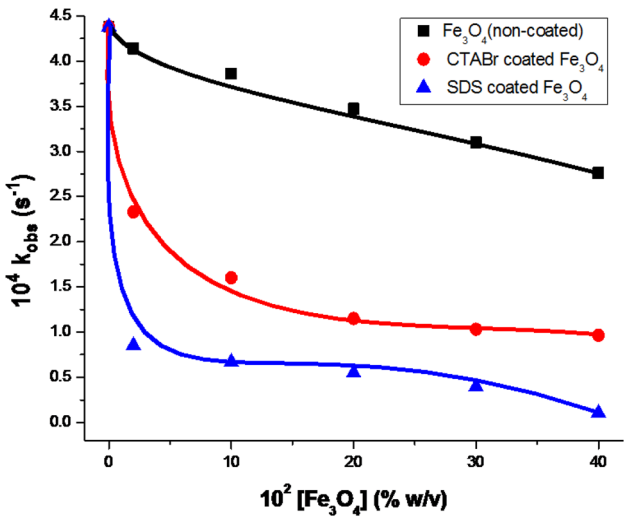

Fig. 10 Plot of observed values of rate constant (k_{obs}) versus [Fe_3O_4]/[surfactant-coated Fe_3O_4]. Reaction conditions: [procaine] = 5.0×10^{-5} mol dm^{-3}, TEMPERATURE = 37 °C

Table 4 Values of K_e obtained from the plots of $\frac{1}{k'_w - k_{SPION}}$ *versus* $\frac{1}{[Surf-SPION]}$

Surfactant–SPIONs	K_e
CTABr–SPION	29.6
SDS–SPION	59.6

Reaction conditions: [procaine] = 5.0×10^{-5} mol dm^{-3} [NaOH] = 5.0×10^{-2} mol dm^{-3} and temperature = 37 °C

Conclusion

The rate of hydrolysis of procaine depends linearly on the concentration of NaOH in the absence and presence of SPIONs but was found to be independent on the initial [procaine]. The addition of surfactants (CTABr and SDS) decreased the rate of hydrolysis of procaine in the presence of SPIONs. The SPIONs coated with CTABr and SDS also decrease the rate of hydrolysis of procaine. The adsorption of procaine to the SPIONs and surfactant-coated SPIONs' surfaces causes a fall on the rate of hydrolysis. The binding constants for procaine–SPIONs were determined based on the pseudophase model and were found to be higher for the surfactant-coated SPIONs than bare SPIONs.

Author contribution Authors Kashif Raees and Mohd Shaban Ansari are the Ph.D students working in the Department of Applied Chemistry, Aligarh Muslim University, Aligarh, India, under the supervision of Prof. M. Z. A. Rafiquee who is also the corresponding author of the paper.

References

1. Alishiri, T., Oskooei, H.A., Heravi, M.M.: Fe_3O_4 nanoparticles as an efficient and magnetically recoverable catalyst for the synthesis of α, β-unsaturated heterocyclic and cyclic ketones under solvent-free conditions. Synth. Commun. **43**, 3357–3362 (2013)
2. Godoi, M., Liz, D.G., Ricardo, E.W., Rocha, M.S.T., Azeredo, J.B., Braga, A.L.: Magnetite (Fe_3O_4) nanoparticles: an efficient and recoverable catalyst for the synthesis of alkynyl chalcogenides (selenides and tellurides) from terminal acetylenes and diorganyl dichalcogenides. Tetrahedron **70**, 3349–3354 (2014)

3. Kumar, A., Gupta, M.: Synthesis and surface engineering of iron oxide nanoparticles for biomedical applications. Biomaterials **26**, 3995–4021 (2005)
4. Azharuddin, M., Tsuda, H., Wu, S., Sasaoka, E.: Catalytic decomposition of biomass tars with iron oxide catalysts. Fuel **87**, 451–459 (2008)
5. Philippot, G., Elissalde, C., Maglione, M., Aymonier, C.: Supercritical fluid technology: a reliable process for high quality. Adv. Powder Technol. **25**, 1415–1429 (2014)
6. Nikitin, A., Fedorova, M., Naumenko, V., Shchetinin, I., Abakumov, M., Erofeev, A., Gorelkin, P., Meshkov, G., Beloglazkina, E., Ivanenkov, Y., Klyachko, N., Golovin, Y., Savchenko, A., Majouga, A.: Synthesis, characterization and MRI application of magnetite water-soluble cubic nanoparticles. J. Magn. Magn. Mater. **441**, 6–13 (2017)
7. Yue-jian, C., Fei, X., Jia-bi, Z., Ning, G., Yi-hua, Z.: Synthesis, self-assembly, and characterization of PEG-coated iron oxide nanoparticles as potential MRI contrast agent. Drug Dev. Ind. Pharm. **36**, 1235–1244 (2010)
8. Cole, A.J., David, A.E., Wang, J., Galbán, C.J., Hill, H.L., Yang, V.C.: Polyethylene glycol modified, cross-linked starch-coated iron oxide nanoparticles for enhanced magnetic tumor targeting. Biomaterials **32**, 2183–2193 (2011)
9. Gupta, A.K., Curtis, A.S.G.: Surface modified superparamagnetic nanoparticles for drug delivery: interaction studies with human fibroblasts in culture. J. Mater. Sci. Mater. Med. **15**, 493–496 (2004)
10. Alexiou, C., Arnold, W., Klein, R.J., Parak, F.G., Hulin, P., Bergemann, C., Erhardt, W., Wagenpfeil, S., Lübbe, A.S.: Locoregional cancer treatment with magnetic drug targeting. Cancer Res. **60**, 6641–6648 (2000)
11. Illés, E., Tombácz, E., Szekeres, M., Tóth, I.Y., Szabó, Á., Iván, B.: Novel carboxylated PEG-coating on magnetite nanoparticles designed for biomedical applications. J. Magn. Magn. Mater. **380**, 132–139 (2015)
12. Illes, E., Szekeres, M., Kupcsik, E., Toth, I.Y., Farkas, K., Jedlovszky-Hajdu, A., Tombacz, E.: PEGylation of surfacted magnetite core-shell nanoparticles for biomedical application. Colloids Surfaces A Physicochem. Eng. Asp. **460**, 429–440 (2014)
13. Pham, X.N., Nguyen, T.P., Pham, T.N., Thuy, T., Tran, N., Tran, T.V.T.: Synthesis and characterization of chitosan- coated magnetite nanoparticles and their application in curcumin drug delivery. Adv. Nat. Sci: Nanosci. Nanotechnol. **7**, 045010 (2016)
14. Kievit, B.F.M., Veiseh, O., Bhattarai, N., Fang, C., Gunn, W., Lee, D., Ellenbogen, R.G., Olson, J.M.: PEI–PEG–chitosan-copolymer-coated Iron oxide nanoparticles for safe gene delivery: synthesis, complexation, and transfection. Adv. Funct. Mater. **19**, 2244–2251 (2009)
15. Sanchez, L.M., Martin, D.A., Alvarez, V.A., Gonzalez, J.S.: Polyacrylic acid-coated iron oxide magnetic nanoparticles: the polymer molecular weight influence. Colloids Surfaces A Physicochem. Eng. Asp. **543**, 28–37 (2018)
16. Couto, D., Freitas, M., Vilas-Boas, V., Dias, I., Porto, G., Lopez-Quintela, M.A., Rivas, J., Freitas, P., Carvalho, F., Fernandes, E.: Interaction of polyacrylic acid coated and non-coated iron oxide nanoparticles with human neutrophils. Toxicol. Lett. **225**, 57–65 (2014)
17. Wu, W., He, Q., Jiang, C.: Magnetic iron oxide nanoparticles: synthesis and surface functionalization strategies. Nanoscale Res. Lett. **3**, 397–415 (2008)
18. Araujo-neto, R.P., Silva-freitas, E.L., Carvalho, J.F., Pontes, T.R.F., Silva, K.L., Damasceno, I.H.M., Egito, E.S.T., Dantas, A.L., Morales, M.A., Carrico, A.S.: Monodisperse sodium oleate coated magnetite high susceptibility nanoparticles for hyperthermia applications. J. Magn. Magn. Mater. **364**, 72–79 (2014)
19. Gawande, M.B., Rathi, A., Nogueira, I.D., Ghumman, C.A.A., Bundaleski, N.: A recyclable ferrite—co magnetic nanocatalyst for the oxidation of alcohols to carbonyl compounds. ChemPlusChem **77**, 865–871 (2012)
20. Teja, A.S., Koh, P.: Synthesis, properties, and applications of magnetic iron oxide nanoparticles. Progr. Cryst. Growth Charact. Mater. **55**, 22–45 (2009)
21. Mamani, J.B., Gamarra, L.F.: Synthesis and Characterization of Fe_3O_4 nanoparticles with perspectives in biomedical applications. Mater. Res. **17**, 542–549 (2014)
22. Marquez, F., Campo, T., Cotto, M., Polanco, R., Roque, R., Fierro, P., Sanz, J.M., Elizalde, E., Morant, C.: Synthesis and characterization of monodisperse magnetite hollow microspheres. Soft Nanosci Lett. **1**, 25–32 (2011)
23. Shen, L., Qiao, Y., Guo, Y., Meng, S., Yang, G., Wu, M., Zhao, J.: Facile co-precipitation synthesis of shape-controlled magnetite nanoparticles. Ceram. Int. **40**, 1519–1524 (2013)
24. Lu, Y., Yin, Y., Mayers, B.T., Xia, Y.: Modifying the Surface Properties of Superparamagnetic Iron Oxide Nanoparticles through A Sol-Gel Approach. Nano Lett. **2**, 183–186 (2002)
25. Schramm, L.L., Stasiuk, E.N., Marangoni, D.G.: Surfactants and their applications. Annu. Rep. Progr. Chem. Sect. C. **99**, 3–48 (2003)
26. Loucas, S.P., Maager, P., Mehl, B.: Effect of procaine on the pH of buffered and unbuffered cardioplegic solutions. Am. J. Hosp. Pharm. **43**, 2213–2218 (1986)
27. Reichert, M.G., Butterworth, J.: Local anesthetic additives to increase stability and prevent organism growth. Tech. Reg. Anesth. Pain Manag. **8**, 106–109 (2004)
28. Philip, J., Chandra, P., Bhagi, R.: X-ray diffraction-based characterization of magnetite nanoparticles in presence of goethite and correlation with magnetic properties. Physica E **39**, 20–25 (2007)
29. Saranya, T., Parasuraman, K., Anbarasu, M., Balamurugan, K.: XRD, FT-IR and SEM study of magnetite (Fe_3O_4) nanoparticles prepared by hydrothermal method. Nano Vision. **5**, 149–154 (2015)
30. Aliramaji, S., Zamanian, A., Sohrabijam, Z.: Characterization and synthesis of magnetite nanoparticles by innovative sonochemical method. Proc. Mater. Sci. **11**, 265–269 (2015)
31. Mahmoudi, M., Simchi, A., Imani, M., Ha, U.O.: Superparamagnetic iron oxide nanoparticles with rigid cross-linked polyethylene glycol fumarate coating for application in imaging and drug delivery. J. Phys. Chem. C **113**, 8124–8131 (2009)
32. Al-Blewi, F.F., Al-Lohedan, H.A., Rafiquee, M.Z.A., Issa, Z.A.: Kinetics of hydrolysis of procaine in aqueous and micellar media. Int. J. Chem. Kinet. **45**, 1–9 (2013)
33. Ansari, M.S., Raees, K., Rafiquee, M.Z.A.: Influence of surfactants/polyethylene glycols mixture on the kinetics of alkaline hydrolysis of tetracaine. J. Mol. Liq. **272**, 638–644 (2018)
34. Raees, K., Ansari, M.S., Rafiquee, M.Z.A.: Synergistic influence of inhibition of PEG-surfactant on the rate of alkaline hydrolysis of procaine. J. Mol. Liq. **257**, 93–99 (2018)
35. Azum, N., Asiri, A.M., Rub, M.A., Al-Youbi, A.O., Khan, A.: Thermodynamic aspects of polymer–surfactant interactions: Gemini (16-5-16)-PVP-water system. Arab. J. Chem. **9**, S1660–S1664 (2016)
36. Singh, S., Dosani, T., Karakoti, A.S., Kumar, A., Seal, S., Self, W.T.: A phosphate dependent shift in Redox state of cerium oxide nanoparticles and its effects on catalytic properties. Biomaterials **32**, 6745–6753 (2011)

Affiliations

Kashif Raees[1] · Mohd Shaban Ansari[1] · M. Z. A. Rafiquee[1]

✉ M. Z. A. Rafiquee
drrafiquee@yahoo.com

[1] Department of Applied Chemistry, Zakir Hussain College of Engineering and Technology, Aligarh Muslim University, Aligarh, UP 202002, India